A matrix-free Model Order Reduction scheme for vibro-acoustic problems with complex damping treatments

S. Jonckheere [1,2], X. Li [3], W. Desmet [1,2]
[1] KU Leuven, Department of Mechanical engineering
Celestijnenlaan 300b, Box 2420, B-3001 Leuven, Belgium
e-mail: **stijn.jonckheere@kuleuven.be**

[2] Member of Flanders Make

[3] Beijing Municipal Institute of Labor Protection
Taoranting Road 55, Beijing 100054, China

Abstract
As the high computational cost hampers simulation over large frequency bands, the current generation of CAE tools, such as the Finite Element Method (FEM), struggles. This problem becomes even worse in the presence of damping treatments. Many Model Order Reduction (MOR) techniques have been developed to alleviate the overall computational load of numerical simulations. Most of them, however, struggle with the complex, and especially frequency dependent properties of typical damping materials. To overcome this problem, a matrix-free technique is proposed. This method is a rational Krylov approach as it uses forced responses to span the projection subspace to reduce the model. As its name ("matrix-free") suggests, it does not require explicit knowledge on the model matrices; the method works on any black-box transfer function between a given number of inputs and outputs. As such, it is a promising technique to speed up vibro-acoustic calculations, even in the presence of damping materials with frequency dependent properties.

1 Introduction

In recent years, the vibro-acoustic performance of products has become a key design feature. This evolution has been instigated by growing customer expectations, as the sound of a product is associated with a certain quality, and by ever tightening regulations on the noise emission levels of products and the human exposure to noise and vibrations. A second, parallel trend, fuelled by an increasing ecological awareness and high direct and indirect material costs, leads to an increased use of lightweight materials. These lightweight materials, however, have less favourable vibro-acoustic properties because of their lower weight with retained stiffness. To mitigate these problems, often multi-layered damping treatments are added, but almost always *a posteriori*, to solve occurring problems. Bringing these damping treatments into an integrated design procedure with often conflicting design requirements, including the NVH (Noise, Vibration and Harshness) behaviour, thus puts design engineers worldwide to the challenge.

A modern design environment requires a lot of prototyping. In order to decrease the time-to-market, the use of virtual prototypes, based on Computer Aided Engineering (CAE) tools, is increasingly the norm. Unfortunately, the current techniques for vibro-acoustic simulation are limited to the low frequency range characterised by long wavelengths relative to the problem geometry due to more than linearly increasing model sizes and simulation times. The introduction of lightweight materials and materials with damping treatments with even shorter characteristic wavelengths even further limits the applicability of classical CAE techniques.

In order to alleviate these problems, a variety of model order reduction (MOR) techniques have been used and developed for decades. Typically, they can be divided into two main groups: (i) modal and (ii) non modal techniques. The conventional modal reduction techniques apply a modal decomposition of the

system. In the special case of the Component Mode Synthesis approach [1], these modes are complemented with static deformation shapes to account for interaction with the boundaries. The second group are the non-modal reduction techniques, which can be further subdivided into Krylov subspace methods, which rely on a polynomial expansion to approximate the matrix inverse using the system's responses as a projection base [2], and the truncation methods, such as balanced truncation [3] and Proper Orthogonal Decomposition (POD) [4], which rely on a singular value decomposition. Many of these methods, however, still struggle with frequency dependencies in the models, such as frequency dependent material properties.

This contribution proposes the use of a method from the family of Krylov methods and discusses a robust reduction scheme which, contrarily to conventional Krylov methods, doesn't require knowledge on the underlying mathematical model, and can hence be considered "matrix-free" [5]; the method only requires knowledge about the transfer function between the system input(s) and output(s). Moreover, problems with frequency dependent material parameters are treated exactly the same as problems with constant properties; the material properties are implicitly included in the transfer functions.

After this introductory section, the paper details the basic theory behind the matrix-free method and its iterative adaptation scheme based on error residuals. An alternative selection criterion for this adaptive rule is proposed based on the relative error between two iterations. Finally, the method is applied on two numerical illustrations considering two types of complex damping treatments: a plate structure with a viscoelastic add-on layer and an acoustic cavity with a porous floor treatment.

2 The matrix-free method

The matrix-free method [5] is the focus of this section. As indicated in the introduction, the method is a Krylov-type MOR technique in that it uses forced responses of the system to span a projection subspace which is used to project the full model on. Contrarily to conventional Krylov approaches, however, the method does not require any detailed knowledge of the underlying mathematical (or other) model equations; the reduced order model (ROM) is built up using explicit transfer functions that are known in a limited number of frequencies. In case additional information is available or can be generated from a (black-box) model, though, an iterative enrichment of the subspace can be performed.

This section firstly discusses the theory behind the matrix-free method and how the ROM is built up from forced responses. Thereafter, the adaptive selection procedure will be discussed together with the associated convergence criteria. Finally, an alternative selection criterion for new frequency lines, based on the relative error between two subsequent ROM, is presented.

2.1 Theory

Consider a general, steady-state dynamic equation in matrix notation:

$$[-\omega^2\mathbf{M}(\omega) + \mathbf{K}(\omega)]\mathbf{x}(\omega) = \mathbf{F}(\omega)\,, \tag{1}$$

where **M** represents the (complex) mass matrix, which is in this case governed by the inertial properties, and **K** the complex stiffness matrix, incorporating the elastic properties. The vector **x** is the vector of unknowns and **F** describes the excitation vector, or when there are a number of different load cases, the excitation matrix. The pulsation ω is directly related to the frequency through $\omega = 2\pi f$.

This general equation (1) returns in many forms, depending on the type of physics that is modelled, such as e.g. structural dynamics, acoustics or coupled vibro-acoustics. For simplicity, we will use the notation in (1)

This general steady-state dynamic equation can be straightforwardly converted into a linear, time-invariant (LTI) state-space notation where **H** represents the matrix of transfer functions between m output points for each of n load cases:

$$\mathbf{H}(\omega) = \mathbf{L}^{\mathrm{T}}[-\omega^2\mathbf{M}(\omega) + \mathbf{K}(\omega)]^{-1}\mathbf{R}, \tag{2}$$

where **L** and **R** are the input and output matrices of size N x m and N x n, respectively.

The calculation of **H** involves an inverse of the dynamic matrix. This matrix, however, can easily describe the dynamic behaviour of models of a few million degrees of freedom in case of a Finite Element (FE) model. Therefore, the matrix inversion can be very expensive, especially because it needs to be repeated at every frequency line. To relieve the associated computational effort, the LTI model is projected onto a Krylov subspace. The left and right projection subspaces are defined as:

$$\bigcup_{\omega\in\Omega_i}\left[(-\omega^2\widehat{\mathbf{M}}+\widehat{\mathbf{K}})^{-\mathrm{T}}\mathbf{L}\right]\subseteq\mathbf{colsp}(\mathbf{W})\,, \tag{3}$$

$$\bigcup_{\omega\in\Omega_j}\left[(-\omega^2\widehat{\mathbf{M}}+\widehat{\mathbf{K}})^{-1}\mathbf{R}\right]\subseteq\mathbf{colsp}(\mathbf{V})\,, \tag{4}$$

where sets Ω_i and Ω_j are two disjoint sets of interpolation frequencies to generate the subspaces. The **colsp**(□)-operator denotes the subspace spanned by a set of column vectors □. The LTI transfer function (3) can then be projected, following the Krylov approach, onto these two subspaces. This results in a ROM with the following approximation for the transfer function:

$$\widehat{\mathbf{H}}(\omega)=\hat{\mathbf{L}}^T\left(-\omega^2\widehat{\mathbf{M}}+\widehat{\mathbf{K}}\right)^{-1}\widehat{\mathbf{R}}\,, \tag{5}$$

where

$$\widehat{\mathbf{K}}=\mathbf{W}^T\mathbf{K}\mathbf{V}\,, \tag{6}$$

$$\widehat{\mathbf{M}}=\mathbf{W}^T\mathbf{M}\mathbf{V}\,, \tag{7}$$

$$\widehat{\mathbf{R}}=\mathbf{W}^T\mathbf{R}\,, \tag{8}$$

$$\hat{\mathbf{L}}=\mathbf{V}^T\mathbf{L}\,. \tag{9}$$

The new transfer function $\widehat{\mathbf{H}}$ interpolates the original transfer function **H**, using the forced responses at the frequencies $\Omega=\Omega_i\cup\Omega_j$. However, in practice often the explicit form of the LTI system (3) is not available such as in the case of indirect modelling approaches like the Boundary Element Method [6] or the Wave Based Method [7,8], or when the outputs are generated by a black-box model. In those cases, the ROM cannot be directly constructed from equations (7)-(10).

To overcome this, a matrix-free formulation of the rational Krylov projection was developed. With $\mathbf{W}_i$ defined as the left projection subspace corresponding to the interpolation frequencies $\omega_i\in\Omega_i$, and $\mathbf{V}_j$ defined as the right projection subspace corresponding to the interpolation frequencies $\omega_j\in\Omega_j$, the (i,j)-th block of the ROM system matrices $\widehat{\mathbf{K}}$ and $\widehat{\mathbf{M}}$ and ROM input- and output matrices $\hat{\mathbf{L}}$ and $\widehat{\mathbf{R}}$ can be calculated as:

$$\widehat{\mathbf{K}}_{ij}=\mathbf{W}_i^{\mathrm{T}}\mathbf{K}\mathbf{V}_j=\frac{\omega_i^2\mathbf{H}(\omega_i)-\omega_j^2\mathbf{H}(\omega_j)}{\omega_i^2-\omega_j^2}\,, \tag{10}$$

$$\widehat{\mathbf{M}}_{ij}=\mathbf{W}_i^{\mathrm{T}}\mathbf{M}\mathbf{V}_j=\frac{\mathbf{H}(\omega_i)-\mathbf{H}(\omega_j)}{\omega_i^2-\omega_j^2}\,, \tag{11}$$

$$\widehat{\mathbf{R}}_i=\mathbf{W}_i^{\mathrm{T}}\mathbf{R}=\mathbf{H}(\omega_i)\,, \tag{12}$$

$$\hat{\mathbf{L}}_j^{\mathbf{T}}=\mathbf{L}^{\mathrm{T}}\mathbf{V}_j=\mathbf{H}(\omega_j)\,. \tag{13}$$

Using these four expressions, the ROM can be directly constructed from the explicit transfer functions $\mathbf{H}(\omega_i)$ with $\omega_i\in\Omega_i$, and $\mathbf{H}(\omega_j)$ with $\omega_j\in\Omega_j$.

The calculation of the ROM approximation $\widehat{\mathbf{H}}$ of the transfer function then directly follows from (6). This can be typically done very cheaply as the ROM typically involves a low (<100) number of degrees of freedom.

2.2 Adaptive interpolation

The quality of the ROM that is produced by the procedure presented in Section 2.1 largely depends on the number and placement of the interpolation frequencies. Through an adaptive procedure, the quality of the ROM can be improved iteratively by adding information from those frequency lines where the approximation error is the largest. Important in this procedure, however, is to have a representative error estimation that is computationally cheap, i.e. that only requires operations on the ROM and not on the full model.

Starting from the transfer function of the original system (3) and of the ROM (6), the approximation error ϵ and the associated residuals vectors $\mathbf{r}_\mathrm{l}$ and $\mathbf{r}_\mathrm{r}$ can be defined, following the theorem proven by Grimme [2], as:

$$\epsilon(\omega) \equiv \mathbf{H}(\omega) - \widehat{\mathbf{H}}(\omega) = \mathbf{r}_\mathrm{l}^\mathrm{T}[-\omega^2\widehat{\mathbf{M}} + \widehat{\mathbf{K}}]^{-1}\mathbf{r}_\mathrm{r}\,, \tag{14}$$

where

$$\mathbf{r}_\mathrm{l}^T(\omega) = \mathbf{L} - [-\omega^2\mathbf{M} + \mathbf{K}]\mathbf{W}[-\omega^2\widehat{\mathbf{M}} + \widehat{\mathbf{K}}]^{-1}\hat{\mathbf{L}}\,, \tag{15}$$

$$\mathbf{r}_\mathrm{r}(\omega) = \mathbf{R} - [-\omega^2\mathbf{M} + \mathbf{K}]\mathbf{V}[-\omega^2\widehat{\mathbf{M}} + \widehat{\mathbf{K}}]^{-1}\widehat{\mathbf{R}}\,. \tag{16}$$

Since evaluating ϵ is as difficult as solving the seed transfer function of the original system, it is proposed to use the residual vectors $\mathbf{r}_\mathrm{l}$ and $\mathbf{r}_\mathrm{r}$ instead [2]. These vectors are not a direct estimation of the modelling error, but do provide some information at which frequencies the error might be large. After application of the matrix-free algorithm, alternative expressions for the residual vectors can be derived that allow to split up the residual vectors in the product of a frequency-independent matrix and a frequency-dependent vector function. The frequency-dependent part is cheap to calculate as it only involves inversions of the ROM system matrices [5]:

$$\mathbf{r}_{\mathrm{l,f}}^T(\omega) = (\omega_\mathrm{i}^2 - \omega^2)[\widehat{\mathbf{K}} - \omega^2\widehat{\mathbf{M}}]^{-1}\hat{\mathbf{L}}\,, \tag{17}$$

$$\mathbf{r}_{\mathrm{r,f}}(\omega) = (\omega_\mathrm{j}^2 - \omega^2)[\widehat{\mathbf{K}} - \omega^2\widehat{\mathbf{M}}]^{-1}\widehat{\mathbf{R}}\,. \tag{18}$$

Based on this criterion, new frequency lines are selected to enrich the ROM in the next iteration. This selection is done in a cascading way: (i) the frequency of the maximum error is selected, (ii) the direct vicinity of the new frequency line is masked to avoid selecting neighbouring maxima, thus to spread out the new frequency lines a bit, (iii) from the remaining frequencies the one corresponding to the new maximum error is selected and the procedure continues along (ii)-(iii) until the requested number of additional frequency lines is reached.

2.3 Convergence

In order to terminate the adaptive procedure once the requested accuracy is reached, a number of criteria are defined to assess the convergence of the method.

The first is the relative error between the ROM approximation $\widehat{\mathrm{H}}$ of the transfer function for two subsequent ROM $\mathrm{n}-1$ and n:

$$\varepsilon_{\mathrm{ROM,ROM}} = \max_\omega \left| \frac{\widehat{\mathrm{H}}_\mathrm{n}(\omega) - \widehat{\mathrm{H}}_{\mathrm{n}-1}(\omega)}{\widehat{\mathrm{H}}_\mathrm{n}(\omega)} \right| < \text{tolerance}\,. \tag{19}$$

The calculation of the transfer function $\widehat{H}$, and subsequently the calculation of the relative error $\varepsilon_{ROM,ROM}$ is computationally cheap.

However, in some cases, the relative error between two subsequent approximations can cause premature termination of the algorithm in case the newly added frequencies are close to the frequencies added in the previous iteration and bring limited additional information to the interpolation. Therefore, another convergence criterion is embedded by comparing the (approximated) transfer function obtained using the current ROM with the (exact) transfer function, calculated with by solving the full system, at the newly selected frequency lines ω_n:

$$\varepsilon_{ROM,Full} = \max_{\omega_n} \left| \frac{\widehat{H}_n(\omega_n) - H_n(\omega_n)}{\widehat{H}_n(\omega_n)} \right| < \text{tolerance}\,. \tag{20}$$

These new frequency lines need to be calculated anyway to build a new ROM in the next iteration. Therefore, also the second relative error criterion $\varepsilon_{ROM,Full}$ has a limited overhead computational cost.

Through this dual error indicator, consisting of the relative error between two subsequent ROM approximations of the transfer function ($\varepsilon_{ROM,ROM}$) and the relative error between the approximated and the exact transfer function in the newly calculated frequency lines ($\varepsilon_{ROM,Full}$), the risk that the algorithm terminates before the requested accuracy is mitigated.

2.4 Alternative frequency selection

Even though the error residual vectors in (18)-(19) give a good estimate for the interpolation error, they have a non-negligible computational cost associated with them. They require an inversion of the reduced matrix for every subspace vector at every iteration. Even though the ROM is generally small, this adds up and creates quite some overhead computations. Moreover, these expressions are only applicable to standard transfer functions; in case one is interested in spatially or frequency integrated values, the error residuals are less meaningful.

Therefore, the relative error between two ROM approximations ($\varepsilon_{ROM,ROM}$ in (20)) is proposed as an alternative function to objectively select the new frequency lines. The calculation of this relative error $\varepsilon_{ROM,ROM}$ is very cheap, as indicated earlier, and is defined directly on the output of interest, the ROM transfer function. Moreover, it is calculated anyway to assess the convergence, and as such brings no overhead to the frequency selection.

One risk in the use of $\varepsilon_{ROM,ROM}$, however, is frequency clustering in case newly added frequencies lead to a large difference between $\widehat{H}_n$ and $\widehat{H}_{n-1}$ at these new frequencies. This would cause the adaptive frequency selection to place the new frequencies in the next iteration again close to the previous interpolation frequencies. This can, however, be easily mitigated by selectively masking the direct vicinity of the frequencies added in the previous iteration.

3 Numerical application

In this section, the matrix-free method is applied to two dynamic cases where a damping treatment with frequency-dependent material parameters is included. The first section studies a flat plate with a viscoelastic add-on treatment, the second focuses on an acoustic problem with a porous wall treatment.

3.1 Flat plate with viscoelastic treatment

A flat, thin steel plate (0.5m x 0.35m x 0.0006m) with material properties defined in Table 1 is presented as the first application case (see Figure 1). The plate is excited through its clamped boundaries (green

boundary) with a uniform normal acceleration $a_n = 1 m/s^2$. Due to the symmetry of the problem, only a quarter of the model needs to be considered. On the symmetry edges (red boundary), the proper symmetry boundary conditions are applied ($\theta_n = 0$). This way, the number of degrees of freedom can be limited. Note that due to this symmetry, only the odd modes will be excited.

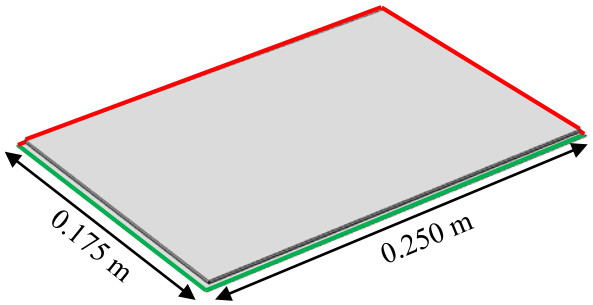

Figure 1: Quarter model of a thin steel plate with a viscoelastic damping treatment.

Steel		
E_s	Young's modulus	210 GPa
η_s	Loss factor	0.1 %
ν_s	Poisson ratio	0.3
ρ_s	Material density	7800 kg/m^3

Table 1: Material properties for steel

The damping treatment (0.49m x 0.34m) is a self-adhesive viscoelastic material layer with a total thickness of 1.5 mm. It is placed centrally on the plate. The material is modelled as a solid with a complex, frequency dependent shear modulus. The material behaviour is described by a Fractional Derivative model [9] using the parameters defined in Table 2, which were derived through inverse characterisation by Rouleau et al. [10]. This material model leads to a frequency dependent storage modulus (real part of the shear modulus) and loss factor (angle of the shear modulus) as shown in Figure 2.

Viscoelastic material [10]		
G_0	Relaxed shear modulus	36.56 kPa
G_∞	Unrelaxed shear modulus	365.6 MPa
α	Order of derivation	0.8
τ	Relaxation time	2.239.10^{-6} s
ρ_v	Material density	1400 kg/m^3
ν_v	Poisson ratio	0.495

Table 2: Viscoelastic material properties for a Fractional Derivatives Model [9]

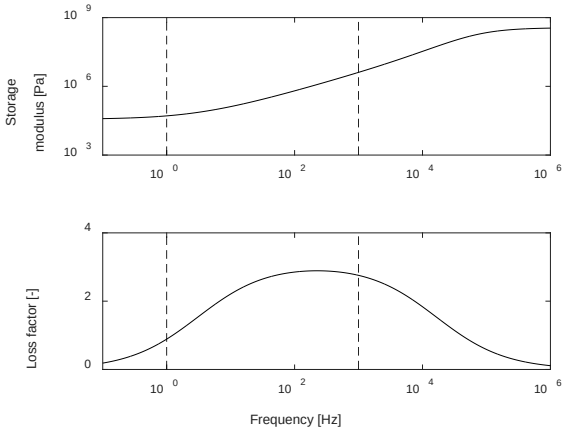

Figure 2: Viscoelastic frequency dependent storage modulus and loss factor from a Fractional Derivatives Model

Three different configurations are considered:

- Bare plate
- Unconstrained damping layer (1.5mm viscoelastic material)
- Constrained damping layer (1.373mm viscoelastic material + 127µm aluminium top sheet)

The acceleration response to the boundary excitation is simulated in the center of the plate, on the untreated side. This is done over a frequency range from 5 Hz to 1000 Hz with a 1 Hz step. The FE models for the three different configurations have 6482, 30231 and 38601 degrees of freedom, respectively. The calculation of one frequency lines took on average 0.12s, 3.7s and 5.4s, respectively, on a Windows 7 laptop with an i7-4600U 2.10 GHz CPU and 16 GB RAM.

Figure 3 shows the acceleration FRF for these three configurations obtained from a full FE simulation. As can be seen in the black curve, the (bare) plate has a moderate modal density; due to the symmetry of the excitation, only 21 out of the 75 modes in the range from 1 to 1000 Hz are excited. When an unconstrained viscoelastic layer is added (red line), the effect on the lower modes is rather limited; the added mass lowers the resonance frequency, but there is hardly any damping. As the frequency increases and the mode shapes become higher dynamic, an increasing amount of shear deformation improves the performance of the viscoelastic layer. Therefore, the resonances of the plate become increasingly damped from 500 Hz onwards. For the third configuration, where the viscoelastic material is constrained by an aluminium top foil (magenta line), the shear deformation of the viscoelastic layer is almost immediately solicited. The plate's resonance frequencies, even the first one, are very efficiently damped out.

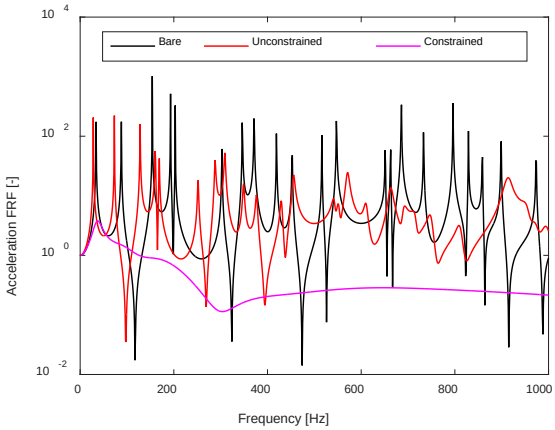

Figure 3: Acceleration FRF for bare and treated plates with boundary excitation.

These transfer functions will now be approximated through the matrix-free method. The method starts with an initial calculation of two frequency lines, setting the boundaries of the frequency range of interest (1 Hz and 1000 Hz). Thereafter, two additional frequency lines are computed and used to build a new ROM. When the requested accuracy of 1% is met, both on $\varepsilon_{ROM,ROM}$ and $\varepsilon_{ROM,Full}$, the algorithm terminates.

Table 3 shows the calculation speed-up for the different configurations, ranging from to 14.7x to 45.5x. In the bare case (Figure 4), the matrix-free method requires 52 full frequency lines to build the reduced model. When an unconstrained treatment is added (Figure 5), this number increases to 68. This can be explained by the fact that the rational interpolation functions require a few more interpolation points (indicated by +) to cope with the increasing degree of damping and smearing of the resonances. Indeed, one can see that more points need to be placed in the damped frequency range from 500 Hz to 1000 Hz as compared to the bare case, whereas this is less outspoken in the range from 1 Hz to 500 Hz. When a constrained layer damping treatment is added (Figure 6), however, most of the modal behaviour is damped out very efficiently. A low number of more or less equally spread out frequency lines suffices.

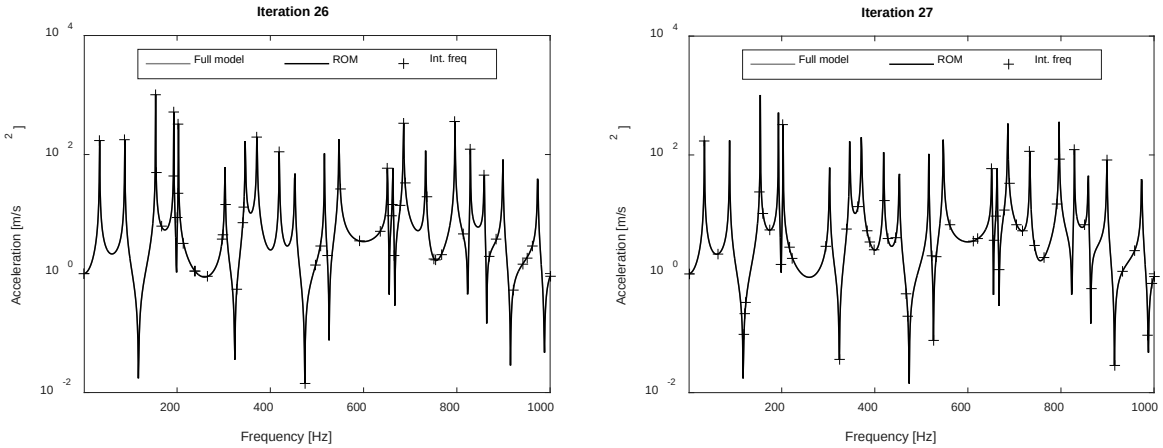

Figure 4: Final approximation for the acceleration transfer function for a bare plate, using (a) error residuals (b) the relative error as a frequency selection criterion

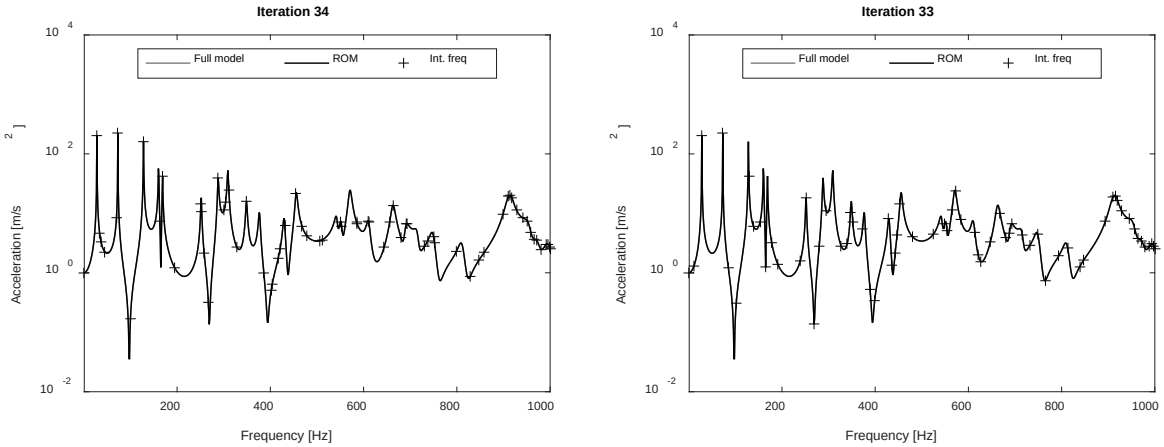

Figure 5: Final approximation for the acceleration transfer function for a plate with an unconstrained viscoelastic treatment, using (a) error residuals (b) the relative error as a frequency selection criterion

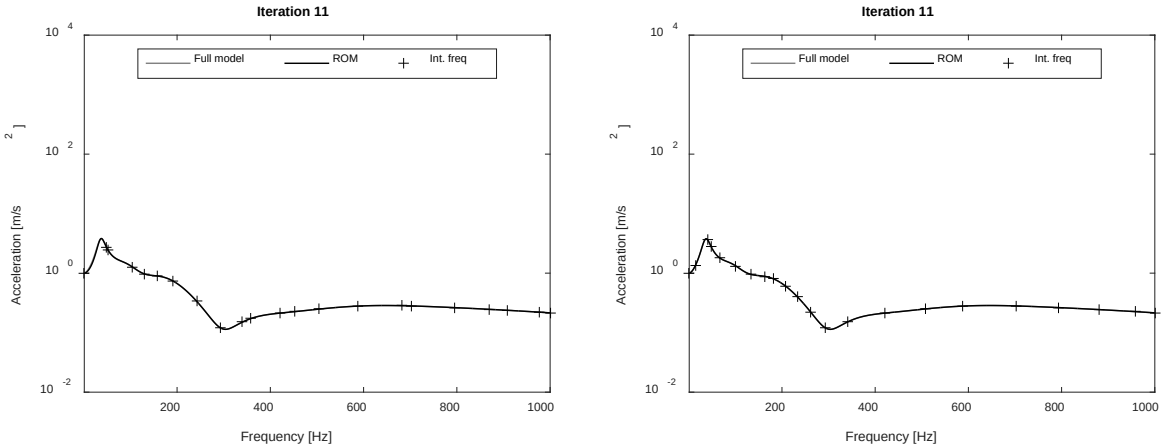

Figure 6: Final approximation for the acceleration transfer function for a plate with a constrained viscoelastic treatment, using (a) error residuals (b) the relative error as a frequency selection criterion

The performance of the relative error based criterion for the selection of new frequency lines in terms of number of iterations (and subsequently in number of frequency lines) holds up well to the error residual based selection. Whereas for the bare configuration, one additional iteration is necessary, one iteration less is required for the unconstrained case. Regarding the overhead, the calculation of the relative error-based

selection criterion, requires less calculation time since this involves criterion almost no additional calculations as the criterion is also used to assess the model's convergence. When using the error residual criterion, however, a number of inversions of the ROM for each of the projection vectors is necessary, leading to a substantial overhead in the same order as the time required for a few frequency lines. This overhead increases further when the size of the ROM increases, and when more iterations are necessary to converge, as can be seen in the comparison between the bare (11.2s overhead) and the unconstrained case (22.9s overhead). Still, even with this overhead the speed-up is remarkable.

		Error residual based criterion				Relative error based criterion			
	Time / freq.	# It.	# Freq.	Speed-up	Error overhead	# It.	# Freq.	Speed-up	Error overhead
Bare	0.12s	26	52	19.2x	11.2s	27	54	18.5x	<0.1s
Unconstrained	3.7s	34	68	14.7x	22.9s	33	66	15.2x	<0.1s
Constrained	5.4s	11	22	45.5x	2.3s	11	22	45.5x	<0.1s

Table 3: Convergence results of the matrix-free approximations for the treated plate configurations

3.2 Acoustic cavity with porous wall treatment

The second application case considers a convex acoustic cavity with non-parallel walls (Figure 7). The cavity corner points are listed in Table 4. The cavity is excited by a loudspeaker (0.15m x 0.1m x 0.15m) located in the back-right-upper corner. The loudspeaker is modelled explicitly as a brick-shaped volume using five rigid boundaries and a vibrating boundary with a prescribed acceleration of $a_n = 1\ m/s^2$ to represent the loudspeaker membrane. The latter is indicated in blue.

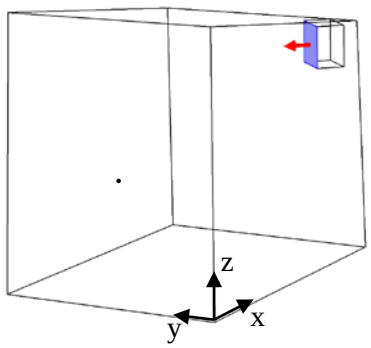

Figure 7: Convex acoustic cavity with non-parallel walls with loudspeaker excitation.

x [m]	y [m]	z [m]
0	0	0
1.15	0	0
1.15	0.815	0
0	0.815	0
0	0.001	0.982
1.082	0.001	0.849
1.082	0.783	0.848
0	0.778	0.981

Table 4: Corner points of the acoustic cavity

The damping treatment is an acoustic treatment in the form of a porous layer with a thickness of 5cm. The material dynamics are approximated using an equivalent fluid model, described by the Johnson-Champoux-Allard [11, 12] model. This means that the skeleton material is assumed rigid, and only the acoustic wave in the interpenetrating fluid is modelled. Therefore, acoustic energy is only dissipated through viscous and thermal interactions of the air inside the material with the skeleton. The material properties for the porous material, which are taken from the thesis of Descheemaeker [13], are given in Table 5. This leads to a complex, frequency dependent bulk modulus and density, as depicted in Figure 8.

Three different configurations with different degrees of damping treatment of the cavity floor are studied:

- Bare cavity (Rigid walls, no damping treatment)
- Partial damping treatment at the center of the floor (0.4m x 0.2m x 0.05m / 9% surface coverage)
- Full damping treatment of the floor (100% floor surface coverage)

The acoustic pressure response is simulated in the point (0.4075m; 0.7856m; 0.2300m) inside the cavity (indicated by ● in Figure 7). The FE models corresponding to each configuration, consisting of 88322, 99941, and 206807 degrees of freedom, respectively. The frequency range from 50 to 600 Hz is simulated with a 0.2 Hz step. The calculation of one frequency lines took on average 12s, 20s and 34s on a Windows 7 laptop with an i7-4600U 2.10 GHz CPU and 16 GB RAM.

Porous material [13]		
ρ_f	Fluid density	1.205 kg/m³
C_p	Heat capacity (p cst.)	1003 J/(kg K)
γ	Specific heat ratio	1.4
k	Thermal conductivity	2.57e-2 W/(m K)
μ	Dynamic viscosity	1.254e-5 Pa s
ϕ	Porosity	0.95
σ	Static flow resistivity	9.2e3 (Pa s)/m²
Λ	Char. viscous length	179e-6 m
Λ'	Char. thermal length	359e-6 m
α_∞	Tortuosity	1.17

Table 5: Porous material properties (Johnson-Champoux Allard model [11,12])

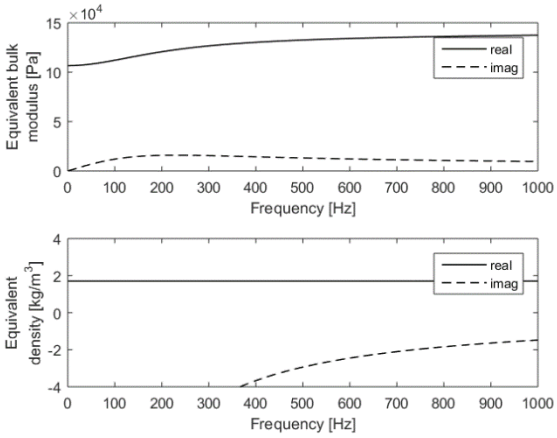

Figure 8: Equivalent fluid frequency dependent bulk modulus and density

Figure 9 shows the dynamic pressure response for these three configurations obtained from a full FE simulation for each case. As can be seen in the black curve, the cavity has a moderate modal density with 28 modes in the range from 50 Hz to 600 Hz. All of them are excited due to the location of the loudspeaker in one of the cavity corners. When a partial porous floor treatment is added (red line), the effect is limited to the higher frequencies due to the relation between the wavelength and the layer dimensions. Nevertheless, due to inertial effects the resonance frequencies shift slightly downwards. When the floor is fully treated (purple line), the impact of the layer increases, and leads to an increased effective mass and damping. Especially the resonance frequencies with a dynamic behaviour normal to the layer are affected and almost entirely damped out. The impact on the modes parallel to the porous layer, on the other hand, is limited.

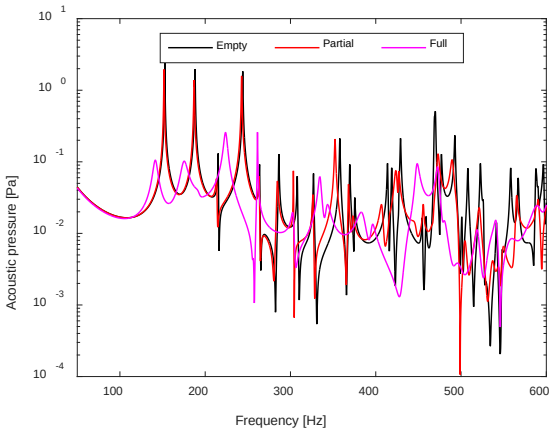

Figure 9: Acoustic pressure response for empty cavity and cavity with partial/full floor treatment with loudspeaker excitation.

Table 6 shows again the calculation speed-up for the different configurations. A speed-up factor between 33.5x and 43.0x can be achieved through application of the matrix-free method with a set tolerance of 1%. As was the case with the treated plate, the most challenging is the approximation of the moderately damped case with a partial floor treatment. Again, the additional frequency evaluations are necessary to capture the damped peaks in the higher frequency range. When more damping material is added, as is the case for a full floor treatment, the dynamic response becomes less modally dominated and the adaptive interpolation requires less interpolation frequencies to converge.

		Error residual based criterion				Relative error based criterion			
	Time / freq.	# It.	# Freq.	Speed-up	Error overhead	# It.	# Freq.	Speed-up	Error overhead
Bare	12s	40	80	34.4x	93.2s	41	82	33.5x	<0.1s
Partial	20s	43	86	32.0x	100s	43	86	32.0x	<0.1s
Full	34s	32	64	43.0x	59.4s	32	64	43.0x	<0.1s

Table 6: Convergence results of the matrix-free approximations for the treated acoustic cavity

In this case, the performance advantage of the relative error based frequency selection comes more clearly to the fore. Because of the higher number of degrees of freedom in the final ROM, the overhead associated with calculating the error residuals, which involves a number of inversions of the subsequent ROMs for the different projection vectors, becomes quite large. Again, the overhead corresponds to the cost of a few frequency line evaluations. The overhead associated with the relative error, however, stays small. Since the number of iterations is roughly the same, the relative error based frequency selection allows to further speed up the matrix-free procedure.

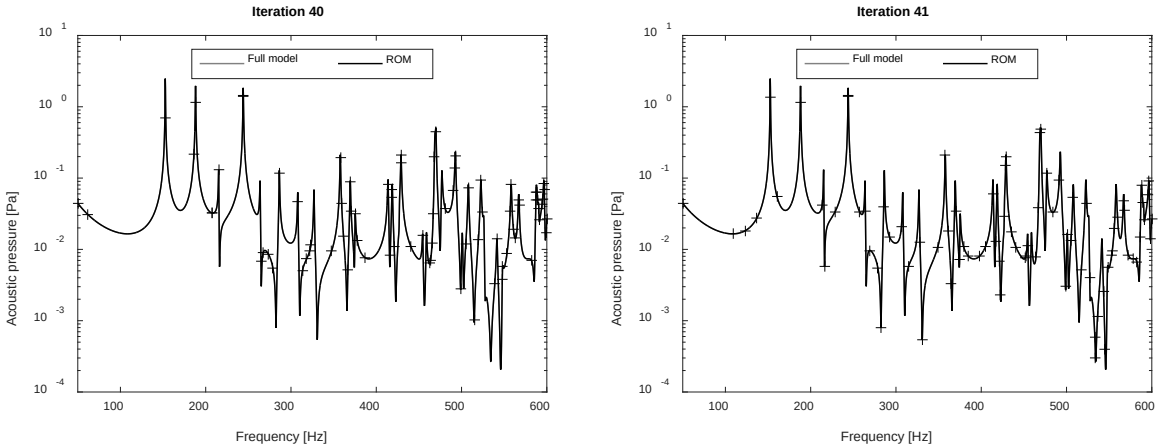

Figure 10: Final approximation for the acceleration transfer function for a bare cavity, using (a) error residuals (b) the relative error as a frequency selection criterion

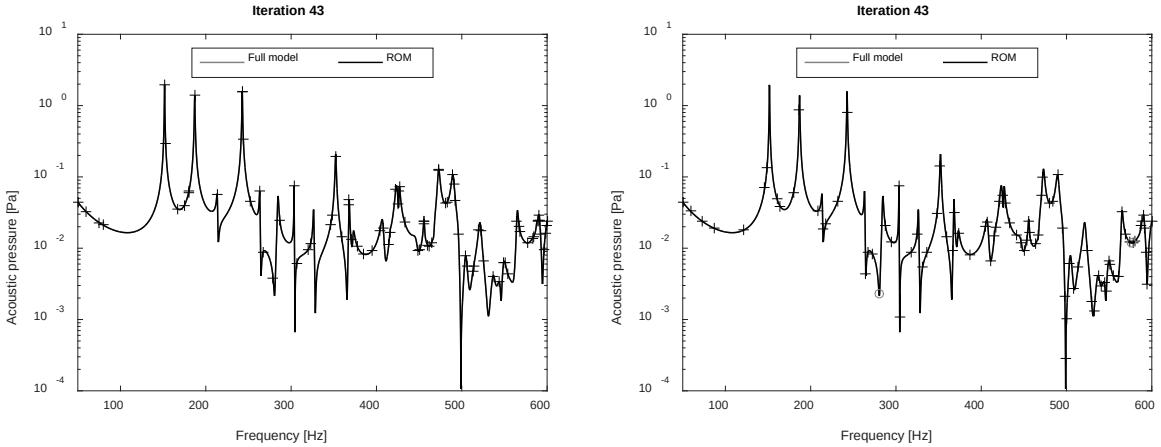

Figure 11: Final approximation for the acceleration transfer function for a cavity with partial floor treatment, using (a) error residuals (b) the relative error as a frequency selection criterion

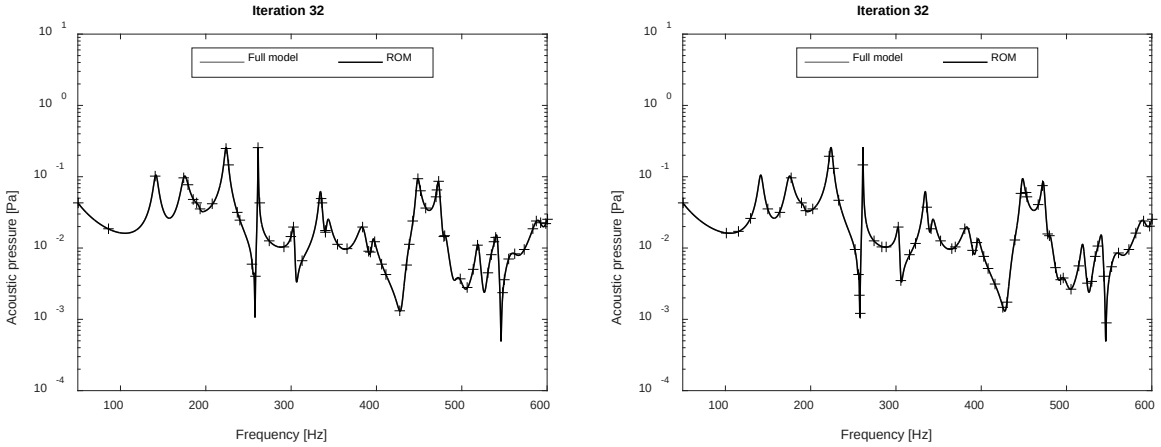

Figure 12: Final approximation for the acceleration transfer function for a cavity with full floor treatment, using (a) error residuals (b) the relative error as a frequency selection criterion

4 Conclusions

To overcome the computational load associated with the direct solution of FE models, especially in the presence of complex damping treatments with frequency-dependent material parameters, a matrix-free implementation of rational Krylov Model Order Reduction was applied. As a “matrix-free” method, it does not require the explicit knowledge of the model matrices, or even of the frequency dependency of the material parameters; it only requires transfer functions between the input(s) and output(s) of interest. As such, it can work on any black-box model, or even experimental data. Moreover, the results can be iteratively improved through an adaptive procedure which uses the error residuals to estimate at which frequencies, the reduced model yields the largest error.

However, there is quite some overhead associated with the calculation of these error residuals. Therefore, another selection criterion is proposed in the form of the relative error between two subsequent approximations of the transfer functions. This way, the overhead is nullified, as this relative error is already calculated to assess the convergence. Moreover, the impact on the number of iterations is negligible and can even reduce the number of iterations in some cases. Finally, this new criterion is more versatile and has the potential to set more complicated targets for the approximation, such as fitting spatial or frequency averaging of the response. This makes the frequency selection criterion matrix-free too; it does no longer require a number of matrix inversions, be it of the ROM.

Finally, the matrix-free algorithm was applied to an acoustic and a structural problem case with various degrees of damping. In all cases, high speed-up factors (10-50x) are obtained, showing the method’s potential to effectively speed up the numerical simulation of undamped, mildly damped and especially heavily damped dynamic problems.

Acknowledgements

The authors gratefully acknowledge SIM (Strategic Initiative Materials in Flanders) and VLAIO (Flanders Innovation & Entrepreneurship) for their support of the ICON project M3NVH, which is part of the research program MacroModelMat (M3). The research of Xianhui Li was supported through NSFC 11174041. The authors would also like to gratefully acknowledge the Research Fund KU Leuven. This research was partially supported by Flanders Make, the strategic research centre for the manufacturing industry.

References

[1] R. J. Craig and M. Bampton, *Coupling of substructures for dynamic analyses*, AIAA Journal 6 (7), 1313-1319, 1968.

[2] E. Grimme, *Krylov projection methods for model reduction*, University of Illinois at Urbana-Champaign PhD thesis, 1997.

[3] B. Moore, *Principal component analysis in linear systems: controlability, observability, and model reduction*, IEEE Transactions on Automatic Control AC-26 (1), 17-32, 1981.

[4] Y. Liang, H. Lee, S. Lim, W.Z., K. Lee and C. Wu, *Proper orthogonal decomposition and its application - Part 1:Theory*, Journal of Sound and Vibration, 252 (3), 44-52, 2002.

[5] X. Li, *Power flow prediction in vibrating systems via model reduction*, Boston University, College of Engineering, Boston, 2004.

[6] O. von Estorff. *Boundary elements in acoustics: Advances and applications*. WITpress, Southampton (United Kingdom), 2000.

[7] E. Deckers, O. Atak, L. Coox, R. D’Amico, H. Devriendt, S. Jonckheere, K. Koo, B. Pluymers, D. Vandepitte, W. Desmet, *The Wave Based Method: an overview of 15 years of research*. Wave Motion 51(4), 550-565, 2014.

[8] S. Jonckheere, *Wave Based and Hybrid Methodologies for Vibro-acoustic Simulation with Complex Damping Treatments*, KU Leuven, Noise &Vibration Research group, PhD thesis, 2015

[9] R.L. Bagley and P.J. Torvik, *A theoretical basis for the application of fractional calculus to viscoelasticity*, Journal of Rheology 27(3), 201-210, 1983.

[10] L. Rouleau, B. Pluymers, W. Desmet, *Characterisation of viscoelastic layers in sandwich lightweight panels through inverse techniques, NOVEM2015 - Noise and vibration, emerging technologies*. Dubrovnik, Croatia, 13-15 April 2015.

[11] D.L. Johnson, J. Koplik, R. Dashen, *Theory of dynamic permeability and tortuosity in fluid-saturated porous media*, Journal of Fluid Mechanics 176, 379-402, 1987.

[12] Y. Champoux and J.-F. Allard, *Dynamic tortuosity and bulk modulus in air-saturated porous media*, Journal of Applied Physics 70(4), 1975-1979, 1991.

[13] J. Descheemaeker. *Elastic characterization of porous materials by surface and guided acoustic wave propagation analysis*, KU Leuven, Department of Physics, PhD thesis, 2011.